Article

Multi-Technique Characterization of Painting Drawings of the Pictorial Cycle at the San Panfilo Church in Tornimparte (AQ)

Francesca Briani [1], Francesco Caridi [2], Francesco Ferella [3], Anna Maria Gueli [4], Francesca Marchegiani [3], Stefano Nisi [3], Giuseppe Paladini [2], Elena Pecchioni [5], Giuseppe Politi [4], Alba Patrizia Santo [5], Giuseppe Stella [4] and Valentina Venuti [2,*]

1   Adarte S.n.c., Via Agnoletti Enriques Annamaria 3, 50141 Firenze, Italy; francescabriani@adartesnc.it
2   Dipartimento di Scienze Matematiche e Informatiche, Scienze Fisiche e Scienze della Terra, Università degli Studi di Messina, V. le F. Stagno D'Alcontres 31, 98166 Messina, Italy; fcaridi@unime.it (F.C.); gpaladini@unime.it (G.P.)
3   CHNet INFN/Laboratori Nazionali del Gran Sasso, Via G. Acitelli 22, Assergi, 67100 L'Aquila, Italy; francesco.ferella@lngs.infn.it (F.F.); francesca.marchegiani@lngs.infn.it (F.M.); stefano.nisi@lngs.infn.it (S.N.)
4   Dipartimento di Fisica e Astronomia "Ettore Majorana", Università degli Studi di Catania, Via S. Sofia 64, 95123 Catania, Italy; anna.gueli@unict.it (A.M.G.); giuseppe.politi@ct.infn.it (G.P.); giuseppe.stella@dfa.unict.it (G.S.)
5   Dipartimento di Scienze della Terra, Università degli Studi di Firenze, Via La Pira 4, 50121 Firenze, Italy; elena.pecchioni@unifi.it (E.P.); alba.santo@unifi.it (A.P.S.)
*   Correspondence: vvenuti@unime.it

Abstract: We present some results, obtained using a multi-scale approach, based on the employment of different and complementary techniques, i.e., Optical Microscopy (OM), Scanning Electron Microscopy-Energy Dispersive X-ray Spectroscopy (SEM-EDS), X-ray diffraction (XRD), Raman and μ-Raman spectroscopy, Fourier transform infrared (FT-IR) spectroscopy equipped with Attenuated Total Reflectance (ATR) analyses, Inductively Coupled Plasma–Mass Spectrometry (ICP-MS), and Thermal Ionization Mass Spectrometry (TIMS), of an integrated activity focused on the characterization of micro-fragments of original and previously restored paintings of the pictorial cycle at the San Panfilo Church in Tornimparte, sampled from specific areas of interest. The study was aimed, on one hand, at the identification of the overlapping restoration materials used during previous conservation interventions (documented and not), and, on the other hand, at understanding the degradation phenomena (current or previous) of the painted surfaces and the architectural structures. The study of stratigraphy allowed us to evaluate the number of layers and the materials (pigments, minerals, and varnishes) present in each layer. As the main result, the identification of blue, black, yellow, and red pigments (both ancient and modern) was achieved. In the case of blue pigments, original (azurite and lazurite) and retouching (Prussian blue and phthalo blue) materials were recognized, together with alteration products (malachite and atacamite). Traces of yellow ochre were found in the yellow areas, and carbon black in the blue and brown areas. In the latter, hematite and red ochre pigments were also recognized. The obtained results are crucial to support the methodological choices during the restoration intervention of the site, and help to ensure the compatibility principles of the materials on which a correct conservative approach is based.

Keywords: San Panfilo Church; multi-scale approach; frescoes; pigments; degradation phenomena; restoration

1. Introduction

The Italian Association of Archaeometry (AIAr) stipulated a Scientific Agreement with the Regional Secretariat of the Ministry of Cultural Heritage and Activities and Tourism for Abruzzo a few years ago. The initiative, launched in collaboration with the Superintendency of Archaeology, Fine Arts and Landscape for the City of L'Aquila and the

municipalities of the Crater, is aimed at the archaeometric study of an important cycle of frescoes in the Church of San Panfilo in Tornimparte (AQ), created along the vault and the perimeter walls of the apse by Saturnino Gatti (1491–1494), a pupil of Verrocchio, and his collaborators [1]. The cycle of frescoes depicts stories from the life and passion of Christ. In particular, in the middle of the vault, a colorful representation of Paradise is symbolized, with the Eternal Father surrounded by Angels and the Blessed. In the arch above the main altar, the Prophets, who foretold the coming of the Redeemer, are depicted, with the Archangel Gabriel in the act of announcing the birth of the Son of God to the Virgin on the sides. Around the apse, in five panels, the moments of the Redemption are reproduced upon a basement of painted marble, i.e.: "*Bacio di Giuda e la Cattura di Cristo*", "*Flagellazione e l'Incoronazione di Spine*", "*Crocifissione*", "*Compianto sul Cristo morto*", and "*Resurrezione*".

The study intends to provide useful information from both a purely cognitive point of view, as a deepening of the artistic technique of the painter and his collaborators, and from a conservative point of view, in order to guide the methodological approaches for the restoration intervention of the site, helping restorers in applying a conservative approach that can guarantee reversibility and compatibility of the used materials [2–10].

The research project proposed by AIAr, by the title "*Studio archeometrico del ciclo pittorico di Saturnino Gatti e bottega presso la chiesa di San Panfilo in Villagrande di Tornimparte (AQ)*", shared and approved with the stipulation of the aforementioned Scientific Agreement, foresees the achievement of the various objectives, including the compositional characterization of the original and restoration materials in view of the identification of the executive technique, and the documentation and understanding of the degradation phenomena, current or past, of the pictorial surfaces and the underlying architectural structures [11–16].

With this aim in mind, the present paper reports the results of a joint investigation focused on the multi-technique characterization of micro-fragments, taken from previously selected areas, using Optical Microscopy (OM), Scanning Electron Microscopy-Energy Dispersive X-ray Spectroscopy (SEM-EDS), X-ray diffraction (XRD), Raman and μ-Raman spectroscopy, Fourier transform infrared (FT-IR) spectroscopy equipped with Attenuated Total Reflectance (ATR) analyses, Inductively Coupled Plasma–Mass Spectrometry (ICP-MS), and Thermal Ionization Mass Spectrometry (TIMS).

It is worth remarking that, other than supporting the planning of the restoration intervention of the frescoes, these results will contribute to the promotion of this precious cultural asset, still almost unknown from an archaeometric point of view.

This paper contributes to the Special Issue "Results of the II National Research project of AIAr: archaeometric study of the frescoes by Saturnino Gatti and workshop at the church of San Panfilo in Tornimparte (AQ, Italy)" in which the scientific results of the II National Research Project conducted by members of the Italian Association of Archaeometry (AIAr) are discussed and collected.

For in-depth details on the aims of the project, see the introduction of the Special Issue [17].

2. Materials and Methods

2.1. Materials

A total of 15 micro-fragments were investigated, whose description and methods of analysis are reported in Table 1, taken from different sampling areas, namely Panel A "*Il bacio di Giuda e la Cattura di Cristo*", Panel D "*Compianto sul Cristo morto*", and Panel E "*Resurrezione*" (see Figure 1).

Table 1. List of investigated samples, together with the approximate size, sampling area, description, and methods of analysis.

Sample	Size (cm)	Sampling Area	Description	Methods of Analysis
SG_18B	0.5	Panel A	Yellow-orange pictorial layer, whitish preparation/priming sample taken along an existing gap	Raman
SG_19	0.5	Panel A	*Detail of a leaf*—Original area (green pictorial layer on a brown-red layer taken up to white plaster support)	OM, SEM-EDS, XRD
SG_20	0.5	Panel A	Original area (blue pictorial layer on a brown-red layer + fragments of plaster below)	OM, SEM-EDS, XRD
SG_21A	0.6	Panel A	*Blue pattern above the window*—Original area (blue pictorial layer on a brown-red layer + fragments of plaster below)	OM, SEM-EDS, XRD
SG_22	0.6	Panel A	*Sky, green pattern*—Original area (green pictorial layer, due to degradation of an originally light-blue layer, on a red-brown layer (fragments of underlying plaster)	OM, SEM-EDS, XRD
SG_23B	0.6	Panel A	*Sky*—Area with drops and probable alterations (light-blue pictorial layer)	μ-Raman, FT-IR
SG_24	0.5	Panel A	*Landscape, area contiguous to the window*—Brown-green pictorial layer + white preparation/priming taken along a gap	Raman
SG_31	0.5	Panel A	Blue pictorial layer + white preparation/priming and sampling carried out in correspondence with a gap	Raman
SG_25B	0.6	Panel D	*Sky, upper portion*—Blue pictorial layer on a brown-red layer + fragments of plaster below	μ-Raman, FT-IR
SG_27B	0.5	Panel D	Light-blue/yellow pictorial layer + white preparation/priming	Raman
SG_28B	0.6	Panel D	Dark-green pictorial layer + plaster fragments. The area also features glazed pictorial additions	μ-Raman, FT-IR
SG_33	0.6	Panel E	Purple pictorial layer (area affected by protective agents that make the surface shiny with a "wax" effect) + plaster fragments	μ-Raman, FT-IR
SG_45B	0.5	Panel E	*Detail of the drapery of the loincloth of the risen Christ*—White pictorial layer applied on an underlying pictorial surface	ICP-MS, TIMS

2.2. Methods

2.2.1. OM Measurements

The stratigraphic study was carried out on polished cross sections of samples using a ZEISS Axio Scope A1 microscope (Carl Zeiss, Jena, Germany), equipped with a video camera, resolution of 5 megapixels, and image analysis software AxioVision (V1). The analyses were carried out in reflected light (Reflected Light Microscopy, RLM).

2.2.2. SEM-EDS Measurements

The morphological and semi-quantitative microchemical analyses were performed using a SEM-EDS electronic microscope (ZEISS EVO MA 15) (Carl Zeiss, Jena, Germany) with a W-filament equipped with an analysis system in energy dispersion EDS/SDD, Oxford Ultimax 40 (40 mm^2 with resolution 127 eV @5.9 keV) (Oxford Instruments, Abingdon,

UK) and the Aztec 5.0 SP1 software. The measurements were performed on carbon metalized cross sections of the samples under the following operating conditions: accelerating potential of 15 kV, 500 pA beam current, working distance between 9 and 8.5 mm; 20 s live time as an acquisition rate useful for archiving at least 600,000 cts, on co-standard, and process time 4 for point analyses; 500 µs pixel dwell time for recording 1024 × 768 pixel resolution maps. The software for the microanalysis was Aztec 5.0 SP1 software, which uses the XPP matrix correction scheme developed by Pouchou and Pichoir in 1991 [18]. This is a Phi-Rho-Z approach that employs exponentials to describe the shape of the φ(ρz) curve. The XPP matrix correction was chosen because it works well in situations with strong absorption, such as the analysis of light elements in a heavy matrix. The method is a "standardless" quantitative analysis, using pre-purchased standard materials for the calculations. The monitoring of constant analytical conditions (i.e., filament emission) is archived with repeated analyses of a Co-metal standard.
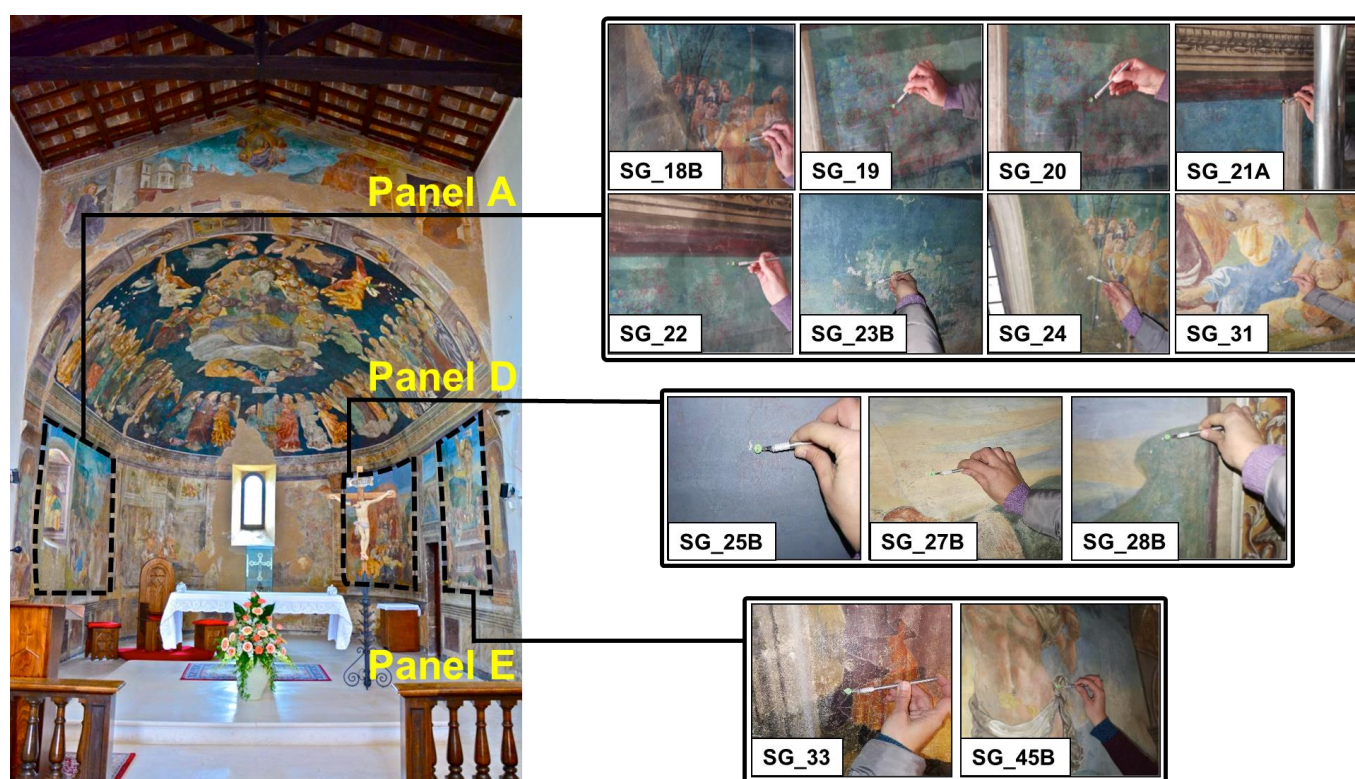

Figure 1. Sampling areas for the investigated micro-fragments.

2.2.3. XRD Measurements

The semi-quantitative mineralogical analyses of the bulk samples were performed using XRD with a Philips PW 1050/37 diffractometer (Philips, Almelo, The Netherlands) and a Philips X'Pert PRO data acquisition and analysis system operating at 40 kV–20 mA, with a Cu anode, a graphite monochromator, and a goniometry speed of 2°/min in a scan range between 5 and 70° θ; the slits are 1-01-1 and the detection limit is 4%.

2.2.4. Raman and µ-Raman Measurements

The raman measurements were performed using a portable Madatech Raman, with a wavelength of 785 nm, a max laser power of 350 mW, an optical-fiber-connected probe head in backscattering geometry, and a Peltier cooled silicon CCD detector. The operative window was 60–3200 cm^{-1} with a resolution of 4 cm^{-1}; the typical acquisition power and time were 30 mW and 30 s, respectively, on a spot of about 2 mm.

The µ-Raman measurements were performed using a portable Raman 'BTR 111 Mini RamTM' (Be&W TEK Inc., Newark, NJ, USA) spectrometer, by using an incident wavelength of 785 nm (diode laser), a max laser power of 280 mW, and a Thermoelectic (CE) Cooled 2048-pixel CCD detector. The 62–3153 cm^{-1} spectral range was investigated, with a resolution of 10 cm^{-1}, an acquisition power of 30 mW and an acquisition time of 10 s × 32 scans. The system was equipped with a BAC151B Raman microscope. The 80× objective, with a working distance of 1.25 mm and a laser beam spot size of 26 µm.

The identification of the peaks was obtained by comparing the experimental spectra with those reported in various databases and the literature [19–22]

2.2.5. FT-IR Measurements

The FT-IR measurements were conducted using a Perkin Elmer Spectrum 100 spectrophotometer, in Attenuated Total Reflectance (ATR) mode, directly on the fragment under examination, without any a priori preparation. The spectra were recorded at a resolution of 4 cm^{-1} between a 500 and 4000 cm^{-1} wavenumber range.

The identification of the peaks was achieved by comparing the experimental spectra with those reported in various databases and in the literature [23,24].

2.2.6. ICP-MS Measurements

The elemental characterization and lead isotope measurement of the sample SG_45B, which was supposed to be "lead white", were performed at the mass spectrometer facility at CHNet-LNGS [25] to study the provenance of the raw material used to produce the pigment. The Inductively Coupled Plasma–Mass Spectrometer (ICP-MS) model 7500a by Agilent Technologies was used for the qualitative elemental characterization. About 5 mg of the sample were dissolved in 5% solution of the nitric acid and properly diluted before instrumental analysis. The concentrations were determined in Semi-quantitative mode calibrating the instrumental response based on a single reference solution containing 10 ng·g^{-1} of Li, Y, Ce, and Tl in order to cover the whole mass range. The uncertainties achieved operating in this mode are about 20% of the concentration value.

2.2.7. TIMS Measurements

The Thermal Ionization Mass Spectrometry (TIMS) is a suitable technique to measure the lead isotope ratio of the sample. The multi-collector spectrometer Finnigan MAT 262 with hardware and software upgraded to TIBox by Spectromat-GmbH (Bremen, Germany) was used [26]. The concentration of Pb measured in the sample using ICP-MS was about 450 mg·kg^{-1}, so its extraction and purification using selective chromatographic resin supplied by Triskem (Bruz, France) was mandatory. Next, 10 mL of the solution and 0.1 M of ammonium oxalate, used to elute the lead from the resin, were evaporated and treated in the oven at 300 °C for 3 h to remove the organic residual. Finally, the lead was recovered using 25 µL of 1% nitric acid solution and then 5 µL were loaded on the "zone-refined" rhenium filament for TIMS measurement.

3. Results and Discussion

3.1. Panel A "Il Bacio di Giuda e la Cattura di Cristo"

In the case of the SG_18B sample, the spectrum obtained from the yellow-orange area (Figure 2) presents two structures, at ~1180 and ~1270 cm^{-1}, that could be attributed to the goethite of yellow ochre; the contribution of this mineral expected at ~440 cm^{-1} is probably masked by the high value of fluorescence, mainly due to the binding media. Additionally, the contribution of calcite, reasonably coming from the preparation layer, is visible.
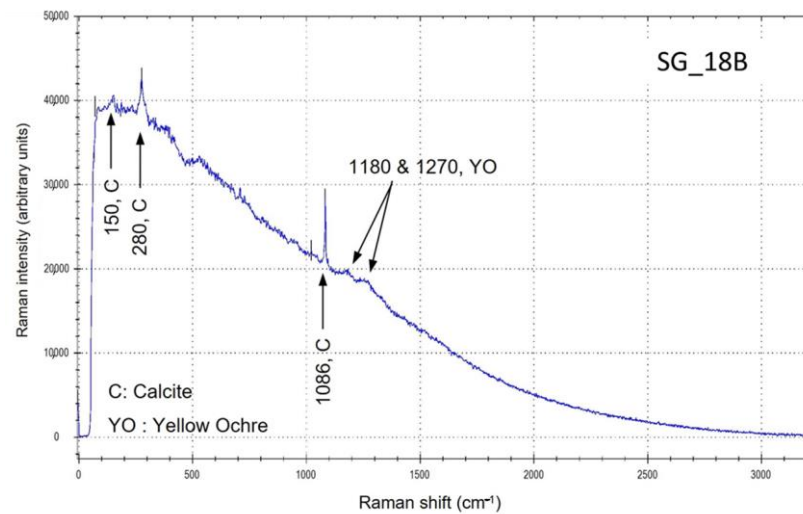
Figure 2. Raman spectrum collected on yellow-orange area of SG_18B sample.

The sample SG_19, collected from a green leaf (Figure 1), shows a four-layer stratigraphy (Figure 3): starting from the surface, we can observe a greenish layer (A) with a thickness of about 25 μm, a blue layer (B), with the same thickness, related to the sky, a red layer (C), and the substrate consisting of the mortar (D). The elemental analysis (SEM-EDS; Table 2) shows the presence of abundant copper in the green and blue grains of the A and B layers, which is due to the use of malachite and azurite pigments. The presence of large amounts of calcium in layers A and B could indicate the use of a white pigment (*Bianco di San Giovanni*?) to lighten the green and blue tones; layer C is made of red ochre film (*morellone*) to protect the pigments from the alkaline effects of the mortar. The XRD analysis of the selected green grains from this sample shows the presence of malachite, along with traces of quartz (Table 3).
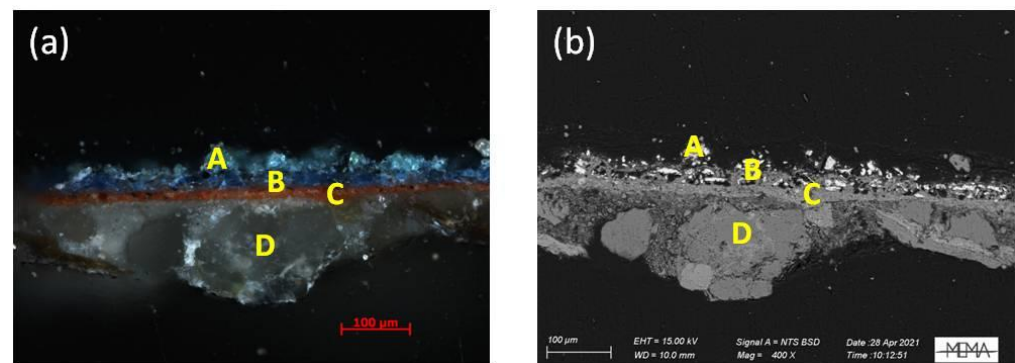

Figure 3. (**a**) Micrographs of SG_19 cross section obtained using OM, showing the four-layer stratigraphy; (**b**) SEM-EDS back-scattering electron image of the four layers.

The sequence of layers of the sample SG_20 (obtained from the base coat of the sky, see Figure 1) consists of only three layers (Figure 4): a very thin (less than 20 μm) blue film (A), a red layer (probably *morellone*) (B), and the mortar substrate (C). The SEM-EDS (Table 2) investigation displays the use of azurite for the outer layer, taking into account the copper content, and red ochre (*morellone*) for the second one. As well as in the sample SG_19, a similar consideration about the presence of a high percentage of calcium in the blue layer is necessary.
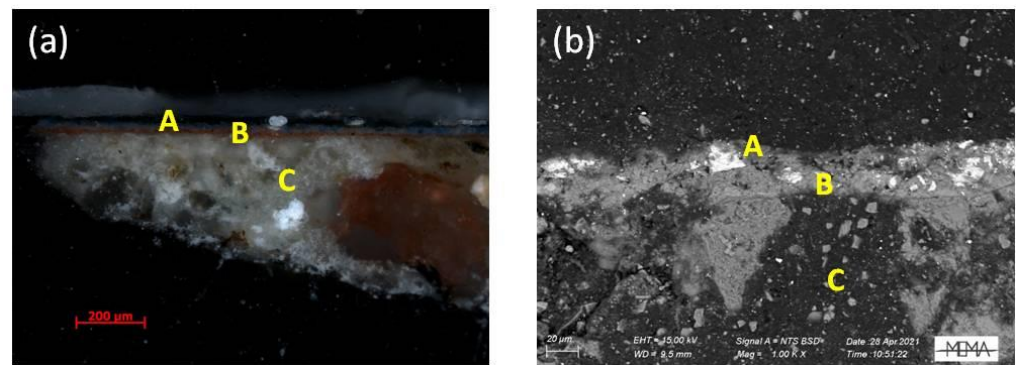
Figure 4. (**a**) Micrographs of SG_20 cross section obtained using OM, showing the three-layer stratigraphy; (**b**) SEM-EDS back-scattering electron image of the three layers.

As for the fragment SG_21A, taken from a blue wash above the window (Figure 1), the observation under the light microscope shows two different shades of blue on the surface (layers A and B), overlying a red layer (C), and the substrate of mortar (D) (Figure 5). The blue layers differ in tonality. The first one (A) is lighter and contains black grains of small size, while the second (B) displays a more intense blue tone and a coarser grain size. In addition, the B layer is not continuous along the section, suggesting a loss of colour from the original film in some areas, and supporting the presence of a secondary integration with the lighter blue pigment belonging to layer A. The SEM-EDS analysis (Table 2) of layer A detected the presence of iron and zinc, suggesting the use of a mixture of Prussian blue and Zinc white. These materials clearly attest to the non-original nature of layer A, allowing us to date the intervention to not before the second half of the XVIII century. The punctual investigation of the black grains observed inside layer A revealed the presence of calcium and phosphorus, due to the use of a bone black pigment, probably added to make the tone of blue darker (too much light), making it uniform with coat B. The elemental analysis confirms the use of azurite for the coarse blue grains of layer B and red ochre for the *morellone* C layer.
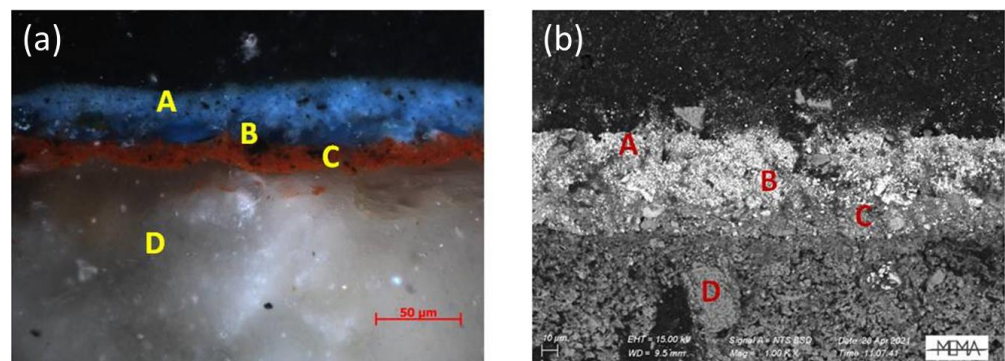

Figure 5. (**a**) Micrographs of SG_21A cross section obtained using OM, showing the four-layer stratigraphy; (**b**) SEM-EDS back-scattering electron image showing the four layers.

The SG_22 greenish fragment was collected from the sky background (Figure 1) that was probably subjected to chromatic alteration. The cross section, observed under the optical microscope, features three layers, including an altered green layer on the surface (A), a thin red layer, probably *morellone* (B), and a substrate consisting of mortar (C) (Figure 6). The SEM-EDS elemental analysis (Table 2) confirms the hypothesis of colour shading in the surface pigment; indeed, copper and chlorine were detected on the A layer, in relation to the formation of atacamite, a copper chloride ($Cu_2Cl(OH)_3$) and a degradation product of azurite. The presence of iron in the red layer attests to the use of the *morellone* (B).
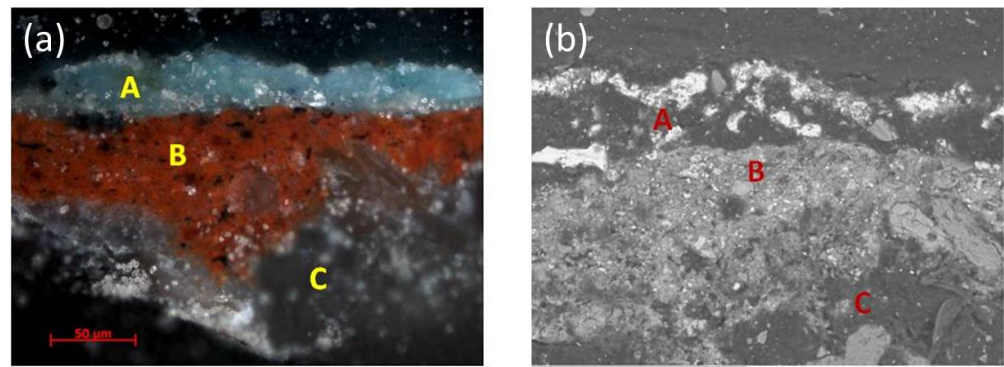
Figure 6. (**a**) Micrographs of SG_22 cross section obtained using OM, showing the three-layer stratigraphy; (**b**) SEM-EDS back-scattering electron image of the three layers.

Table 2. EDS analysis (weight %) of samples SG_19, SG_20, SG_21A, and SG_22 cross sections.

Sample ID	P_2O_5	MgO	Al_2O_3	SiO_2	SO_3	Cl	K_2O	CaO	FeO	CuO	ZnO
SG_19 Greenish layer	-	3.58	1.89	12.33	3.83	-	-	17.75	3.02	55.54	-
SG_19 Blue layer	-	1.84	1.29	13.27	1.96	-	1.38	41.76	3.24	34.50	-
SG_20 Blue layer	-	1.54	-	10.99	2.14	-	0.90	45.24	-	38.48	-
SG_21A A blue layer	-	-	2.01	20.10	3.44	-	-	5.70	2.06	7.49	58.43
SG_21A A layer, black grains	29.93	-	-	-	3.04	-	-	36.19	-	-	30.13
SG_21A B layer, blue grains	-	-	-	-	-	-	-	1.06	-	98.94	-
SG_22 Greenish layer	-	1.86	1.68	4.77	-	24.73	0.63	4.95	-	61.38	-

A supplementary fragment of the sample SG_22 was investigated using XRD (Table 3). The analysis reveals and confirms the presence of atacamite, resulting from azurite alteration under specific conditions; the presence of quartz, calcite, plagioclase, mica, and chlorite are to be attributed to the composition of the mortar that polluted the analysis of the pigment.

Table 3. XRD semi-quantitative results: XXX = high content; XX = medium content; X = low content; tr = traces.

Sample ID	Quartz	Calcite	Plagioclase	Mica	Malachite	Chlorite	Atacamite
SG_19	tr	-	-	-	XXX	-	-
SG_22	XX	X	X	tr	-	tr	tr

In the case of the SG_23B micro-fragment, the μ-Raman spectrum (Figure 7) collected on a blue area shows the presence of lazurite, as a blue pigment, mixed with carbon black (smoke black), calcite, and gypsum. Importantly, considering the specific historical–geographical context and execution technique of the whole pictorial cycle, the presence of gypsum can be considered as intentionally added by the painter as binding material for the pigments. However, the existence of gypsum, resulting from environmentally activated alteration processes that took place over time onto the topmost pictorial surface, cannot be excluded.
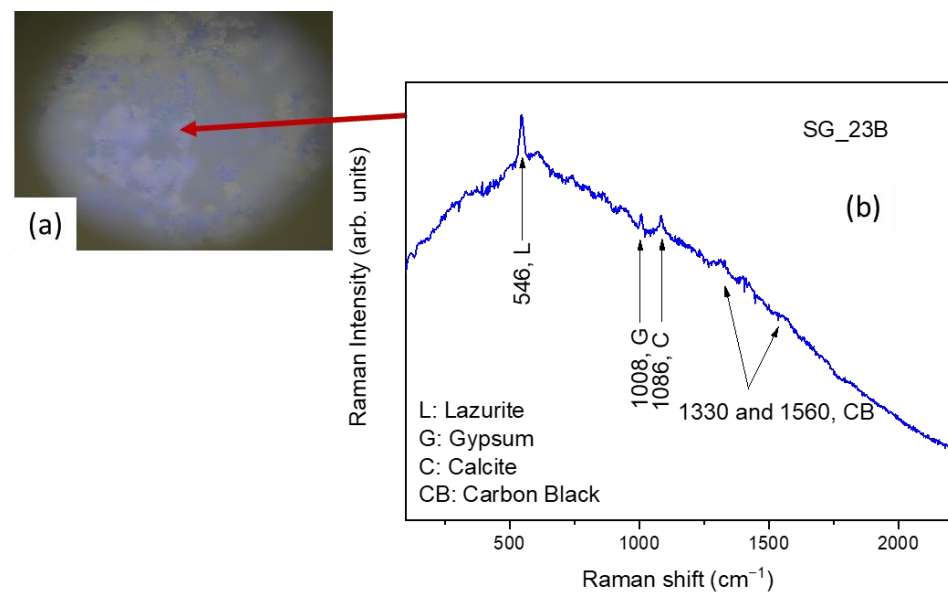
Figure 7. (**a**) Micro-photo of the analyzed blue area, (**b**) μ-Raman spectrum collected on the blue area of SG_23B sample.

The FT-IR spectrum of this sample (Figure 8) clearly highlighted the presence of the characteristic bands of calcite and gypsum. The band between ~890 cm^{-1} and ~1230 cm^{-1} is associated with silicates. No organic binders are observed.
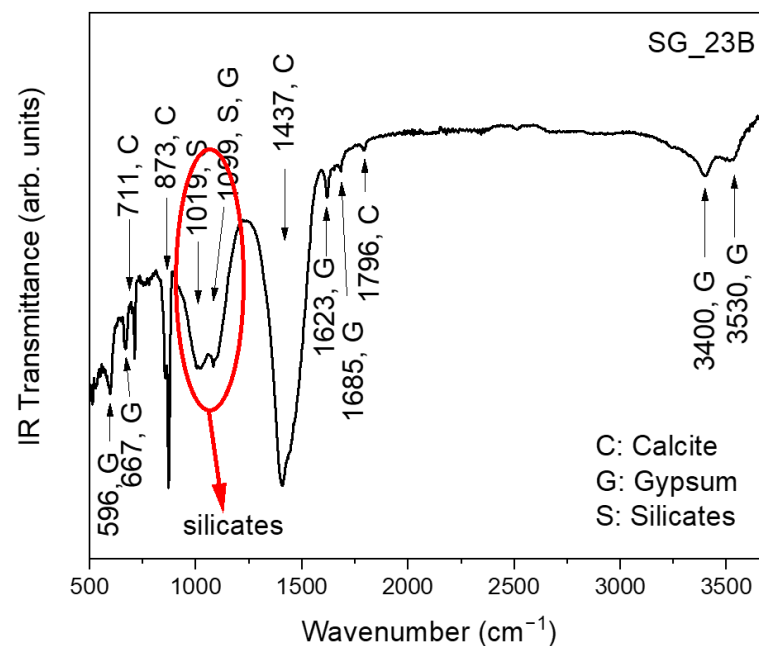

Figure 8. FT-IR spectrum of SG_23B sample.

This experimental evidence is in agreement with the use of the "*a fresco*" technique for the application of the pigment.

The spectrum (Figure 9) measured on the brown-green pictorial layer of SG_24 sample shows the presence of carbon black, probably used to darken the used pigment, that does not show any characteristic peak.
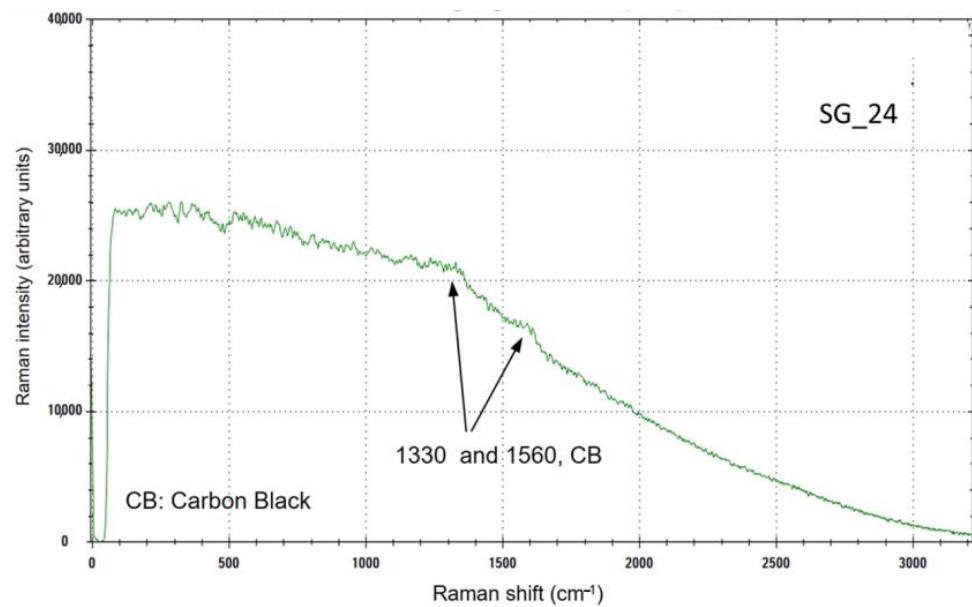
Figure 9. Raman spectrum collected on SG_24 brown-green sample.

The SG_31 blue sample shows a Raman spectrum (Figure 10) with the characteristic peak of calcite and those of carbon black. No marks of a blue pigment are visible.
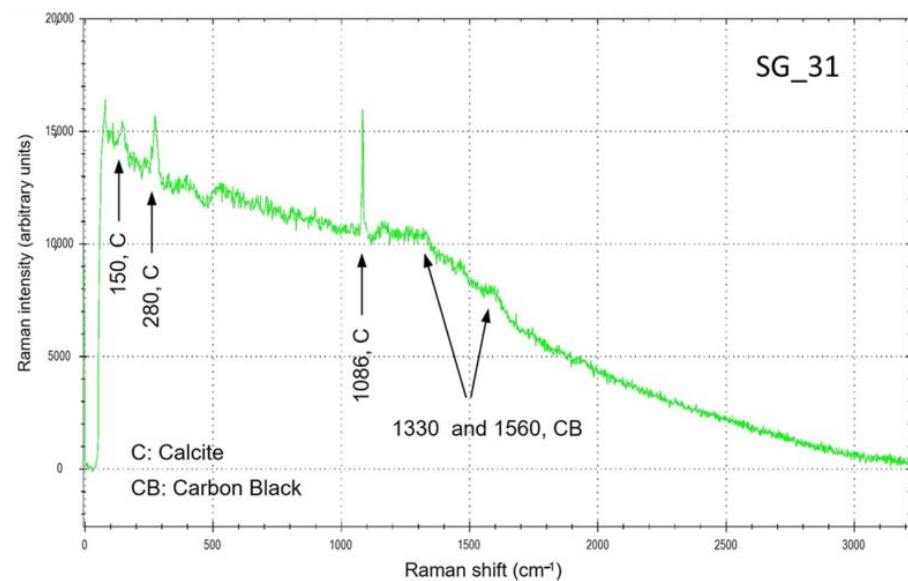

Figure 10. Raman spectrum collected on SG_31 blue sample.

3.2. Panel D "Compianto sul Cristo Morto"

First, a Raman analysis was carried out on a red area (Figure 11a) of the SG_25B micro-fragment, whose spectrum highlighted the presence of calcite and gypsum (Figure 11b). No bands attributable to the pigment were observed. Furthermore, a Raman investigation was carried out on a blue area (Figure 11c), whose spectrum (Figure 11d) allowed for highlighting the presence of lazurite [27,28], as an azure pigment, mixed with phthalo blue (synthetic inorganic pigment), in addition to the peak at 1086 cm^{-1} attributable to the calcite plaster.
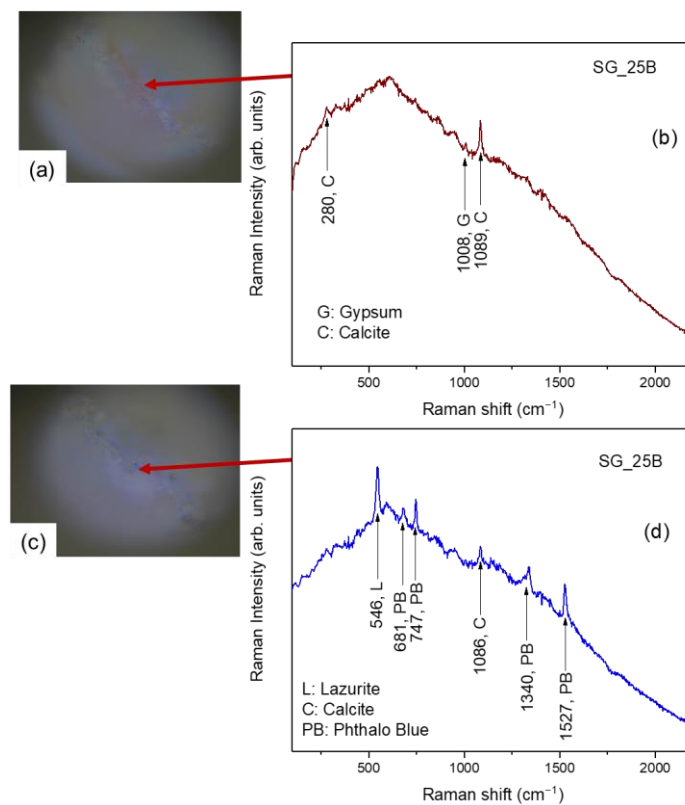
Figure 11. (**a**) Micro-photo of the analyzed red area, (**b**) μ-Raman spectrum collected on the red area of SG_25B sample, (**c**) micro-photo of the analyzed blue area, (**d**) μ-Raman spectrum collected on the blue area of SG_25B sample.

The FT-IR spectrum of the SG_25B sample, reported in Figure 12, appears entirely dominated by the vibrational contributions of calcite and gypsum. No organic binders are observed.
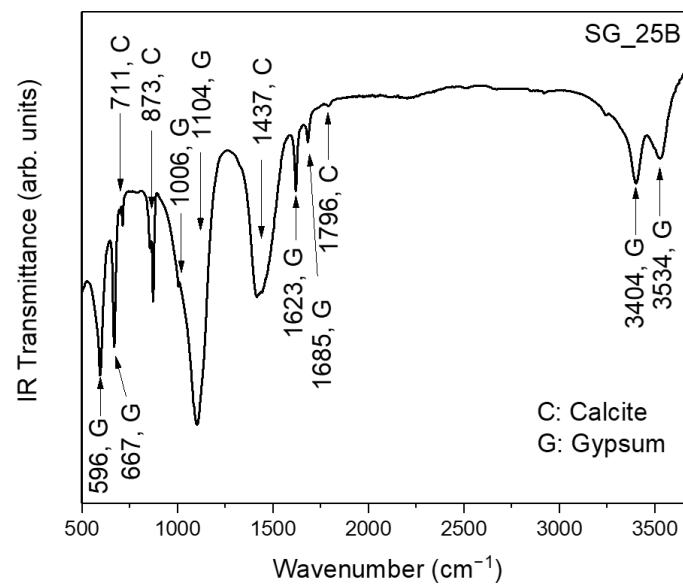

Figure 12. FT-IR spectrum of SG_25B sample.

In the light-blue/yellow area of the SG_27B sample (Figure 13), the Raman spectrum presents the peaks of calcite, and, again, the two structures of yellow ochre. No marks of

a blue pigment, expected with 785 nm excitation laser in the region of 400–600 cm^{-1} for lazurite or azurite, are visible, probably masked by the high fluorescence.
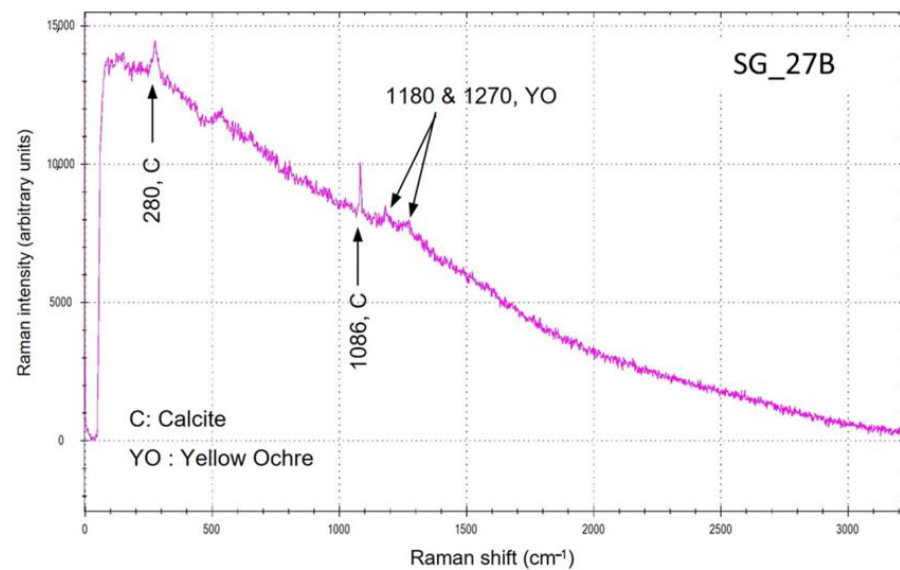

Figure 13. Raman spectrum collected on SG_27B light-blue/-yellow sample.

As regards the SG_28B sample, the μ-Raman observation highlights blue areas (Figure 14a). The spectrum (Figure 14b) exhibits all the characteristic peaks of phthalo blue.
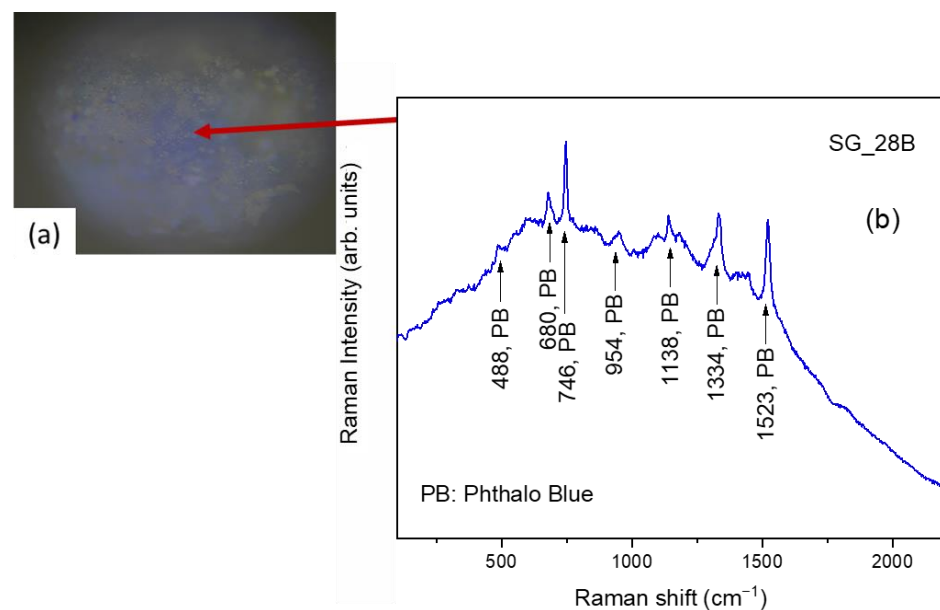

Figure 14. (**a**) Micro-photo of the analyzed blue area, (**b**) μ-Raman spectrum collected on the blue area of SG_28B sample.

The FT-IR spectrum of this sample (Figure 15), in addition to the usual contributions from calcite, highlighted the presence of the broadband between ~890 cm^{-1} and ~1230 cm^{-1} associated with the presence of silicates, together with the contributions at ~1633 cm^{-1} (HOH bending) and the broad band centered at ~3300 cm^{-1} (OH stretching), which is indicative of the presence of clayey minerals. No organic binders are observed.
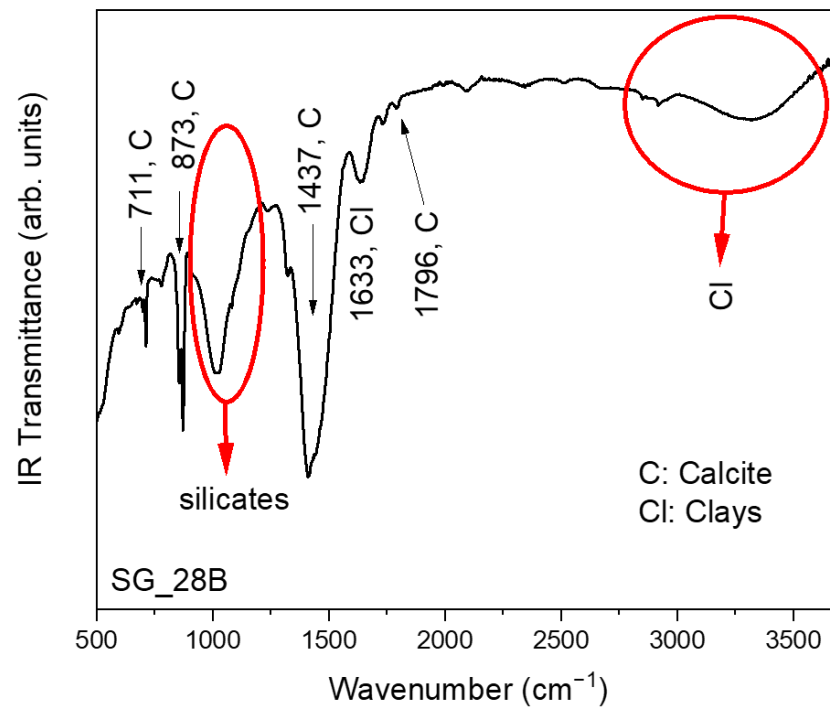
Figure 15. FT-IR spectrum of SG_28B sample.

3.3. Panel E "Resurrezione"

As far as the SG_33 micro-fragment is concerned, the brown area analyzed using μ-Raman (Figure 16) allowed for highlighting all the characteristic peaks of hematite, as a red pigment, mixed with carbon black, as well as calcite from the base.
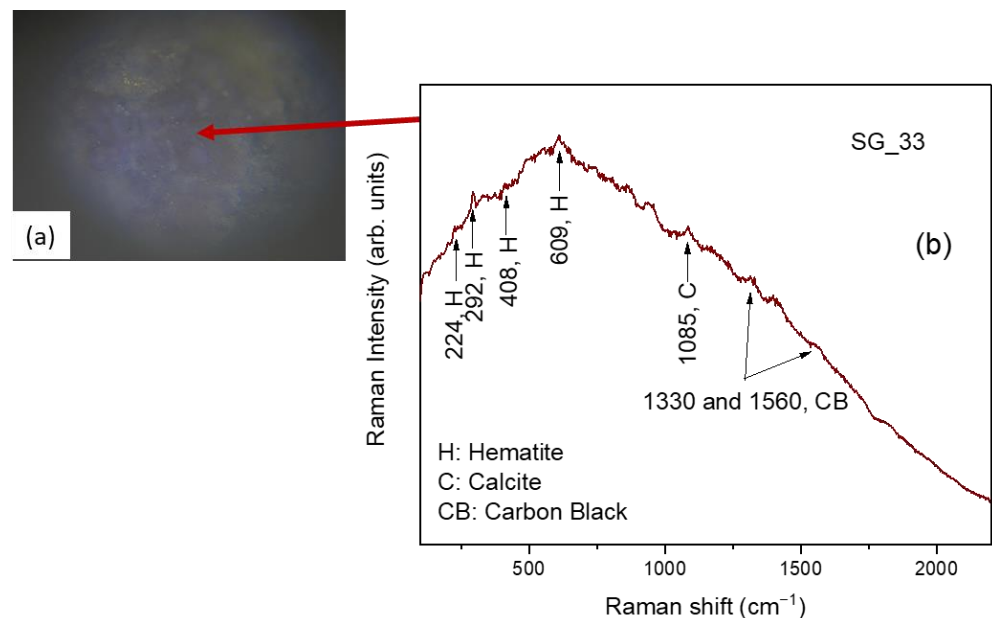

Figure 16. (**a**) Micro-photo of the analyzed brown area, (**b**) μ-Raman spectrum collected on the brown area of SG_33 sample.

The FT-IR spectrum (Figure 17) clearly revealed the presence of the typical vibrational bands of calcite.
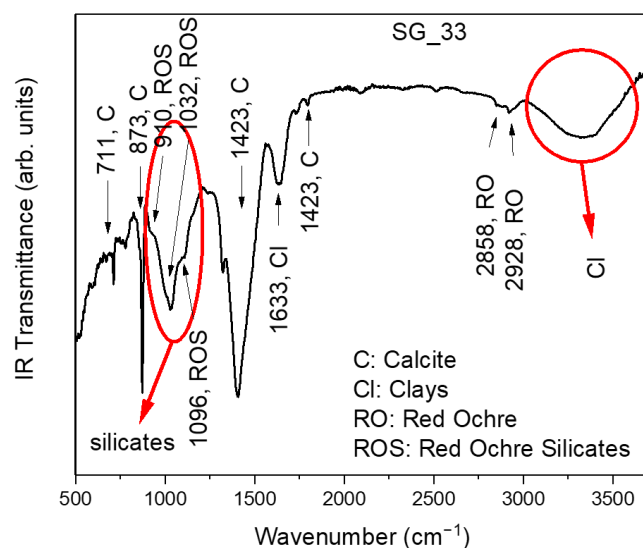
Figure 17. FT-IR spectrum of SG_33 sample.

Again, the broad band between ~890 cm^{-1} and ~1230 cm^{-1} associated with the presence of silicates appears evident. Within it, the peaks at ~910 cm^{-1}, ~1032 cm^{-1}, and ~1096 cm^{-1}, which can be associated to silicates, probably present in red ocher [29], can be distinguished. Finally, the band at ~1633 cm^{-1} and the broad band centered at ~3300 cm^{-1}, attributed to the OH groups, are indicative of the presence of clayey minerals. No organic binders are observed.

The elemental composition of the sample SG_45B was investigated using ICP-MS. The concentrations of the main detected elements are reported in Table 4.

Table 4. Elemental composition of the sample measured using ICP-MS. The uncertainties are 20% of the concentration values.

Sample ID	Element	Concentration [mg·kg^{-1}]	Concentration [%]
	Na	265	0.03
	Mg	2100	0.2
	Ca	62,000	6.2
SG_45B	Fe	1000	0.1
	Cu	74	0.007
	Zn	520	0.05
	Ba	1000	0.1
	Pb	450	0.045

The Pb contained in the sample constitutes a very small mass fraction (0.045%), so the analyzed material cannot be correctly identified using the "lead white" pigment, commonly used in these studies, which contains about 80% of lead. Even if the results allow for a partial identification of the sample, the most abundant compounds seem to be calcium based, such as gypsum or calcite.

The doubtful origin of the lead poses a basic uncertainty to study the provenance of the raw material used in the pictorial layer. Moreover, the availability of a single sample introduces uncertainty about the overall representativeness of the entire painting.

The lead isotope composition measured in the sample is quite rare due to the relatively high value of Pb207/206 and Pb208/206 ratio. Table 5 compares the isotopic ratios measured for SG_45B and those for some mining sites in the South of France that have the closest lead isotope signature related to the sample.

Table 5. Comparison between the lead isotope ratio of SG_45B sample with closest lead mines present in the database.

Sample	$^{207}Pb/^{206}Pb$	$^{208}Pb/^{206}Pb$	$^{206}Pb/^{204}Pb$	$^{207}Pb/^{204}Pb$	$^{208}Pb/^{204}Pb$
SG45B	0.8529 ± 0.0003	2.0900 ± 0.0007	18.26 ± 0.03	15.57 ± 0.03	38.16 ± 0.07
Férols, Montgaillard (France)	0.8525	2.0903	18.33	15.63	38.32
Lastours, Montagne Noire (France)	0.8535	2.0910	18.36	15.67	38.39
Cevennes, Massif Central (France)	0.8519	2.0915	18.36	15.64	38.40

In particular, the Férols mine, located in the region of present-day New Aquitaine, shows reasonable compatibility considering the limits discussed above.

4. Conclusions

In the present study, a multi-scale approach involving Optical Microscopy (OM), Scanning Electron Microscopy-Energy Dispersive X-ray Spectroscopy (SEM-EDS), X-ray diffraction (XRD), Raman and μ-Raman spectroscopy, Fourier transform infrared (FT-IR) spectroscopy equipped with Attenuated Total Reflectance (ATR) analyses, Inductively Coupled Plasma–Mass Spectrometry (ICP-MS), and Thermal Ionization Mass Spectrometry (TIMS) was employed in order to characterize, in the framework of the A.I.Ar. Research project "*Studio archeometrico del ciclo pittorico di Saturnino Gatti e bottega presso la chiesa di San Panfilo in Villagrande di Tornimparte (AQ)*", the micro-fragments of the paintings of the pictorial cycle at the San Panfilo Church in Tornimparte, sampled from specific areas of interest.

Such a combined approach allowed us to successfully characterize, both at the elemental and molecular scales, the composition of the materials used by the artist in terms of preparatory components and pigmenting agents, furnishing novel insights into the execution technique of the master, the color palette, and the occurrence of nondocumented restoration treatments. Moreover, the analysis of the sample stratigraphy permitted a proper evaluation of the number of layers, together with the materials present in each of them. In this context, the measurements allowed us to confirm, among other aspects, the presence of both ancient and modern pigments, together with alteration products onto the pictorial surfaces of the cycle of frescoes.

It is worth noting that the whole set of results, obtained by the employment of a multi-scale approach involving different spatial regimes, represents an essential pre-requisite in view of the optimization of the latest restoration procedures and for the accurate selection, by restorers and conservators, of the protection and best-cleaning strategies to be applied.

Author Contributions: Conceptualization, F.B., F.C., F.F., A.M.G., F.M., S.N., G.P. (Giuseppe Paladini), E.P., G.P. (Giuseppe Politi), A.P.S., G.S. and V.V.; methodology, F.B., F.C., F.F., A.M.G., F.M., S.N., G.P. (Giuseppe Paladini), E.P., G.P. (Giuseppe Politi), A.P.S., G.S. and V.V.; validation, V.V.; formal analysis, F.B., F.C., F.F., A.M.G., F.M., S.N., G.P. (Giuseppe Paladini), E.P., G.P. (Giuseppe Politi), A.P.S., G.S. and V.V.; investigation, F.B., F.C., F.F., A.M.G., F.M., S.N., G.P. (Giuseppe Paladini), E.P., G.P. (Giuseppe Politi), A.P.S., G.S. and V.V.; data curation, F.B., F.C., F.F., A.M.G., F.M., S.N., G.P. (Giuseppe Paladini), E.P., G.P. (Giuseppe Politi), A.P.S., G.S. and V.V.; writing—original draft preparation, F.B., F.C., F.F., A.M.G., F.M., S.N., G.P. (Giuseppe Paladini), E.P., G.P. (Giuseppe Politi), A.P.S., G.S. and V.V.; writing—review and editing, F.B., F.C., F.F., A.M.G., F.M., S.N., G.P. (Giuseppe Paladini), E.P., G.P. (Giuseppe Politi), A.P.S., G.S. and V.V.; visualization, F.B., F.C., F.F., A.M.G., F.M., S.N., G.P. (Giuseppe Paladini), E.P., G.P. (Giuseppe Politi), A.P.S., G.S. and V.V.; supervision, V.V. All authors have read and agreed to the published version of the manuscript.

Institutional Review Board Statement: Not applicable.

Informed Consent Statement: Not applicable.

Data Availability Statement: The data presented in this study are available on request from the corresponding author.

Conflicts of Interest: The authors declare no conflict of interest.

References

1. Latini, M. Chiesa di San Panfilo—Villagrande di Tornimparte (AQ). In *Guida alle Chiese d'Abruzzo*; Carsa Edizioni: Pescara, Italy, 2016; pp. 139–140. ISBN 978-88-501-0354-6.
2. Zuena, M.; Buemi, L.P.; Stringari, L.; Legnaioli, S.; Lorenzetti, G.; Palleschi, V.; Nodari, L.; Tomasin, P. An integrated diagnostic approach to Max Ernst's painting materials in his Attirement of the Bride. *J. Cult. Herit.* **2020**, *43*, 329–337. [CrossRef]
3. Venuti, V.; Fazzari, B.; Crupi, V.; Majolino, D.; Paladini, G.; Morabito, G.; Certo, G.; Lamberto, S.; Giacobbe, L. In situ diagnostic analysis of the XVIII century Madonna della Lettera panel painting (Messina, Italy). *Spectrochim. Acta Part A Mol. Biomol. Spectrosc.* **2020**, *228*, 117822. [CrossRef] [PubMed]
4. Fermo, P.; Mearini, A.; Bonomi, R.; Arrighetti, E.; Comite, V. An integrated analytical approach for the characterization of repainted wooden statues dated to the fifteenth century. *Microchem. J.* **2020**, *157*, 105072. [CrossRef]
5. Castro, K.; Benito, Á.; Martínez-Arkarazo, I.; Etxebarria, N.; Madariaga, J.M. Scientific examination of classic Spanish stamps with colour error, a non-invasive micro-Raman and micro-XRF approach: The King Alfonso XIII (1889–1901 "Pelón") 15 cents definitive issue. *J. Cult. Herit.* **2008**, *9*, 189–195. [CrossRef]
6. La Russa, M.F.; Ruffolo, S.A.; Belfiore, C.M.; Comite, V.; Casoli, A.; Berzioli, M.; Nava, G. A scientific approach to the characterisation of the painting technique of an author: The case of Raffaele Rinaldi. *Appl. Phys. A* **2014**, *114*, 733–740. [CrossRef]
7. Edwards, H.G.M.; Jorge Villar, S.E.; Eremin, K.A. Raman spectroscopic analysis of pigments from dynastic Egyptian funerary artefacts. *J. Raman Spectrosc.* **2004**, *35*, 786–795. [CrossRef]
8. Vizárová, K.; Reháková, M.; Kirschnerová, S.; Peller, A.; Šimon, P.; Mikulášik, R. Stability studies of materials applied in the restoration of a baroque oil painting. *J. Cult. Herit.* **2011**, *12*, 190–195. [CrossRef]
9. Andreotti, A.; Izzo, F.C.; Bonaduce, I. Archaeometric Study of the Mural Paintings by Saturnino Gatti and Workshop in the Church of San Panfilo—Tornimparte (AQ). The Study of Organic Materials. *Appl. Sci.* **2023**. *submitted*.
10. Spoto, S.E.; Paladini, G.; Caridi, F.; Crupi, V.; D'Amico, S.; Majolino, D.; Venuti, V. Multi-Technique Diagnostic Analysis of Plasters and Mortars from the Church of the Annunciation (Tortorici, Sicily). *Materials* **2022**, *15*, 958. [CrossRef]
11. Bonizzoni, L.; Caglio, S.; Galli, A.; Lanteri, L.; Pelosi, C. Materials and Technique: The First Look at Saturnino Gatti. *Appl. Sci.* **2023**. *submitted*.
12. Bonizzoni, L.; Caglio, S.; Galli, A.; Germinario, C.; Izzo, F.; Magrini, D. Identifying Original and Restoration Materials through Spectroscopic Analyses on Saturnino Gatti Mural Paintings: How Far a Non-Invasive Approach can Go. *Appl. Sci.* **2023**. *submitted*.
13. Armetta, F.; Giuffrida, D.; Ponterio, R.C.; Falcon Martinez, M.F.; Briani, F.; Pecchioni, E.; Santo, A.P.; Ciaramitaro, V.C.; Saladino, M.L. Looking for the Original Materials and Evidence of Restoration at the Vault of the San Panfilo Church in Tornimparte (AQ). *Appl. Sci.* **2023**. *submitted*.
14. Ricci, S. Tornimparte, a Mimesis of Florence in Abruzzo. New Insights into Saturnino Gatti's Art. *Appl. Sci.* **2023**. *submitted*.
15. Germinario, L.; Giannossa, L.C.; Lezzerini, M.; Mangone, A.; Mazzoli, C.; Pagnotta, S.; Spampinato, M.; Zoleo, A.; Eramo, G. Petrographic and Chemical Characterization of the Frescoes by Saturnino Gatti (Central Italy, 15th Century): Microstratigraphic Analyses on Thin Sections. *Appl. Sci.* **2023**. *submitted*.
16. Comite, V.; Bergomi, A.; Lombardi, C.A.; Fermo, P. Characterization of Soluble Salts on the Frescoes by Saturnino Gatti in the Church of San Panfilo in Villagrande di Tornimparte (L'Aquila). *Appl. Sci.* **2023**. *submitted*.
17. Galli, A.; Alberghina, M.F.; Re, A.; Magrini, D.; Grifa, C.; Ponterio, R.C.; La Russa, M.F. Special Issue: Results of the II National Research Project of AIAr: Archaeometric Study of the Frescoes by Saturnino Gatti and Workshop at the Church of San Panfilo in Tornimparte (AQ, Italy). *Appl. Sci.* **2023**. *submitted*.
18. Pouchou, J.-L.; Pichoir, F. *Quantitative Analysis of Homogeneous or Stratified Microvolumes Applying the Model "PAP." In Electron Probe Quantitation*; Springer US: Boston, MA, USA, 1991; pp. 31–75.
19. Buzgar, N.; Apopei, A.I.; Buzatu, A. Romanian Database of Raman Spectroscopy. Available online: http://rdrs.uaic.ro (accessed on 9 March 2023).
20. Lafuente, B.; Downs, R.T.; Yang, H.; Stone, N. The power of databases: The RRUFF project. In *Highlights in Mineralogical Crystallography*; Armbruster, T., Danisi, R.M., Eds.; W. De Gruyter: Berlin, Germany, 2015; pp. 1–30. ISBN 9783110417104.
21. Caggiani, M.C.; Cosentino, A.; Mangone, A. Pigments Checker version 3.0, a handy set for conservation scientists: A free online Raman spectra database. *Microchem. J.* **2016**, *129*, 123–132. [CrossRef]
22. Pigments Checker—Modern & Contemporary Art. Available online: http://chsopensource.org/tools-2/pigments-checker/ (accessed on 9 March 2023).
23. De Benedetto, G.E.; Laviano, R.; Sabbatini, L.; Zambonin, P.G. Infrared spectroscopy in the mineralogical characterization of ancient pottery. *J. Cult. Herit.* **2002**, *3*, 177–186. [CrossRef]
24. Sadtler Database for FT-IR. Available online: http://www.ir-spectra.com/sadtler/sadtler.htm (accessed on 7 March 2023).

25. Giuntini, L.; Castelli, L.; Massi, M.; Fedi, M.; Czelusniak, C.; Gelli, N.; Liccioli, L.; Giambi, F.; Ruberto, C.; Mazzinghi, A.; et al. Detectors and Cultural Heritage: The INFN-CHNet Experience. *Appl. Sci.* **2021**, *11*, 3462. [CrossRef]

26. Wegener, M.R.; Mathew, K.J.; Hasozbek, A. The direct total evaporation (DTE) method for TIMS analysis. *J. Radioanal. Nucl. Chem.* **2013**, *296*, 441–445. [CrossRef]

27. Chukanov, N.V.; Vigasina, M.F.; Zubkova, N.V.; Pekov, I.V.; Schäfer, C.; Kasatkin, A.V.; Yapaskurt, V.O.; Pushcharovsky, D.Y. Extra-Framework Content in Sodalite-Group Minerals: Complexity and New Aspects of Its Study Using Infrared and Raman Spectroscopy. *Minerals* **2020**, *10*, 363. [CrossRef]

28. Caggiani, M.C.; Acquafredda, P.; Colomban, P.; Mangone, A. The source of blue colour of archaeological glass and glazes: The Raman spectroscopy/SEM-EDS answers. *J. Raman Spectrosc.* **2014**, *45*, 1251–1259. [CrossRef]

29. Crupi, V.; Fazio, B.; Fiocco, G.; Galli, G.; La Russa, M.F.; Licchelli, M.; Majolino, D.; Malagodi, M.; Ricca, M.; Ruffolo, S.A.; et al. Multi-analytical study of Roman frescoes from Villa dei Quintili (Rome, Italy). *J. Archaeol. Sci. Rep.* **2018**, *21*, 422–432. [CrossRef]